Vol. **107** (2005) *ACTA PHYSICA POLONICA A* No. 4

Proceedings of the 35th Polish Seminar on Positron Annihilation, Turawa, Poland 2004

Sensitivity of Positronium Momentum Distribution to Phase Transitions in Crystalline Dielectrics

I.V. Bondarev[a] and T. Hyodo[b]

[a]The Institute of Nuclear Problems, The Belarusian State University
Bobruiskaya Str. 11, 220050 Minsk, Belarus
[b]Institute of Physics, Graduate School of Arts and Sciences, University of Tokyo
3-8-1 Komaba, Meguro-ku, Tokyo 153-8902, Japan

We give a review of recent theoretical and experimental study of the positronium–phonon and positronium–quadrupole interactions in dielectric crystals of different local symmetries, placing a special emphasis on the sensitivity of the positronium momentum distribution to the second order phase transitions in crystalline dielectrics.

PACS numbers: 78.70.Bj, 71.60.+z, 71.38.–k, 36.10.Dr

1. Introduction

Positronium (Ps), a bound state of an electron and a positron, forms in various dielectric crystals [1]. Being a light impurity atom in a crystal lattice, Ps is extremely sensitive to its local surroundings and phonon lattice vibrations. In crystal lattices of non-cubic symmetry, the Ps atom may exhibit effective quadrupole interactions even in spite of the fact that it is completely electroneutral in vacuum [2]. The Ps effective quadrupole interaction is absent in cubic crystals because of evident symmetry restrictions resulted from the cubic isotropy. Both in cubic and in non-cubic crystals, Ps interacts with phonons in a way different from that the electron does. Namely, the neutral Ps atom intensively interacts with short-range acoustic and optic deformation potentials only, not responding to long-range phonon-induced electric fields [3]. These two circumstances, the effective quadrupole interactions and short-range phonon interactions, make the Ps atom a tool for the study of symmetry-dependent structural properties of Ps-forming crystals.

We give a brief review of recent theoretical and experimental studies of the Ps-phonon and Ps-quadrupole interactions in dielectric crystals of different local symmetries, placing a special emphasis on the sensitivity of the Ps momentum distribution to the second order phase transitions in crystalline dielectrics.

2. Ps states in defectless crystals: delocalized and self-trapped Ps

Positronium has been found to form in a delocalized Bloch-type state in dielectric crystals with low enough concentration of defects (no more than 10^{15} defects per cm^3 [4]) at sufficiently low temperatures (typically below a few tens K) [5]. The formation of Bloch-type Ps in these crystals is confirmed by observing very narrow peaks (the central peak and satellite peaks appearing at the momentum corresponding to the reciprocal lattice vectors of the sample crystal) in the momentum distribution of the photons resulting from the 2γ-decay of Ps upon irradiating the crystals by low-energy positrons. As temperature increases, it is observed that the central Ps peak becomes drastically wider and the satellite peaks disappear, indicating the localization of Ps [5]. Such an effect of a thermally activated self-localization (self-trapping) of Ps was observed in many ionic crystals and was analyzed theoretically in Refs. [6, 7].

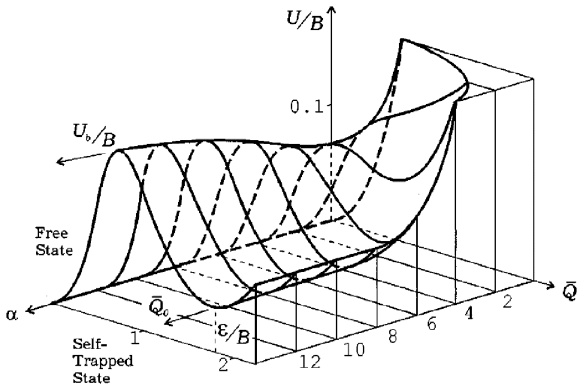

Fig. 1. Dimensionless potential energy surface for the Ps atom in a cubic crystal at zero temperature [6]. B is the half-width of the Ps band in an undistorted lattice, $\overline{Q}$ and α are the dimensionless amplitude and the dimensionless reciprocal radius of the lattice distortion, respectively.

Figure 1 shows a typical zero-temperature potential energy surface versus the amplitude and the reciprocal radius of the lattice distortion for the positronium atom coupled to a field of longitudinal acoustic phonons (acoustic deformation potential) in a cubic crystal [6]. The potential energy has two minima separated by the potential barrier. The minima correspond to the stable delocalized (free) Ps state with no lattice distortion and to the metastable self-trapped Ps state

with a finite lattice distortion, respectively. At very low temperatures, positronium is in the free delocalized state. As temperature increases and becomes of the order of the energy difference between the two states ($\sim$ 0.01 eV in ionic crystals [7]), positronium (together with the lattice, self-consistently) escapes into the self-trapped state by means of the under-barrier tunneling. As this takes place, the self-trapping always dominates over the detrapping back into the free state because of the large number of the trapping sites (of the order of that of the unit cells) in the crystal. At higher temperatures, the tunneling mechanism of the Ps self-trapping is supplemented by the classical surmounting of the potential barrier, so that at room temperature almost all the Ps atoms annihilate from the self-trapped states yielding a broad central peak with no satellite components in the Ps momentum distribution measured.

Below we briefly describe recent theoretical and experimental results for delocalized Ps states in cubic and non-cubic dielectric crystals.

3. Cubic and non-cubic crystals: Ps–phonon and Ps effective quadrupole interactions

The delocalized Ps atom is a light extrinsic impurity in a crystal. Because it is light compared with atoms forming a crystal lattice, it is extremely sensitive to its local crystalline surroundings. In crystal lattices of non-cubic symmetry, Ps may sense intracrystalline electric field gradients on it via an effective quadrupole moment it acquires due to the difference in effective masses of the electron and the positron [2]. Such an effective quadrupole interaction is absent in cubic crystals because of evident symmetry restrictions resulted from the cubic isotropy. However, both in cubic and in non-cubic crystals, Ps may interact with local lattice deformations caused by thermal lattice vibrations (phonons). In so doing, the neutral Ps atom, contrary to a charged electron, does not respond to long-range phonon-induced electric fields and intensively interacts with short-range acoustic and optic deformation potentials only [3].

3.1. Ps effective quadrupole interactions in non-cubic crystals

It is well known that all hydrogen-like atoms consisting of electrically positive and negative particles with different masses possess a quadrupole moment in the ground state due to the electron–nucleus hyperfine interaction. This was first predicted in Ref. [8] and then confirmed by the discovery of the anisotropy of the hyperfine splitting of muonium in α-quartz [9]. Positronium, which is the lightest hydrogen-like atom, does not have any multipole moments in vacuum because of the fundamental restrictions imposed by the CPT-theorem on a quantum system consisting of two particles with charges of opposite signs and equal masses [10]. As a consequence, "vacuum" Ps is a totally CPT-invariant quantum system with identically zero multipole moments. However, Ps in material is a many-particle

system, strictly speaking, which consists of one single positron and many electrons since the electron in Ps is indistinguishable from those in material. Such a quantum system can possess an effective quadrupole moment (the first one of the multipole expansion yielding a non-zero interaction with local electric fields — see, e.g., [11]) as the main initial requirement of the CPT-theorem is now lifted and the effective masses of the electron and the positron are different [12].

Possible manifestations of the Ps effective quadrupole interactions in non--cubic crystals were analyzed in Refs. [13–15]. The effective quadrupole interaction was shown to result in the anisotropy of the Ps magnetic quenching in an external magnetostatic field. In other words, if the crystal is oriented in two different ways with respect to the direction of the magnetic field, then the Ps quadrupole coupling constant can be detected through the measurement of the difference (the anisotropy) of the fraction of Ps atoms which self-annihilate at two different relative orientations of the crystal and the magnetic field applied. Specifically, if θ and φ are the polar and the lateral angles characterizing the tilt of the magnetic field $\boldsymbol{B}$ with respect to the system of principal axes of the tensor V_{ik} of electric field gradients (EFG) in the center of mass of the Ps atom, the intensity $I_{\rm Ps}$ of the central peak of the Ps momentum distribution is given by [15]

$$I_{\rm Ps}(B,\theta,\varphi) \approx \Xi(B,\theta,\varphi) I_{\rm Ps}(0), \tag{1}$$

where $I_{\rm Ps}(0)$ is the Ps peak intensity in the zero magnetic field. The function $\Xi(B,\theta,\varphi)$ has the form

$$\Xi(B,\theta,\varphi) = \frac{1 + 2\frac{\Gamma_0(0)}{\Gamma_1(0)} y_q^2 + 2P y_q}{1 + 2\frac{\Gamma_0(0)}{\Gamma_1(0)} y_q^2}, \tag{2}$$

where P is the projection of the positron polarization vector on the magnetic field direction at the instant of Ps formation,

$$\Gamma_1(B) = \kappa \frac{\gamma_{\rm t} + y_q^2 \gamma_{\rm s}}{1 + y_q^2} + \gamma_{\rm po} \quad \text{and} \quad \Gamma_0(B) = \kappa \frac{y_q^2 \gamma_{\rm t} + \gamma_{\rm s}}{1 + y_q^2} + \gamma_{\rm po} \tag{3}$$

are the total annihilation rates of the *ortho*-like and *para*-like Ps atoms in the crystal in the presence of the magnetostatic field, $\gamma_{\rm s}$ and $\gamma_{\rm t}$ are the self-annihilation rates of the singlet and triplet Ps in vacuum, $\gamma_{\rm po}$ is the Ps peak-off annihilation rate in the crystal, $\kappa = \omega/\omega_0$ is the electron–positron contact density of Ps in the crystal relative to vacuum with ω and $\omega_0 = 8.41 \times 10^{-4}$ eV being the hyperfine splitting frequencies of the Ps ground state in the crystal and in vacuum, respectively. The factor y_q in Eqs. (2) and (3) is of the form

$$y_q = y \sqrt{1 + \frac{d}{\omega} \frac{3\cos^2\theta - 1 + \eta \sin^2\theta \cos 2\varphi}{2\sqrt{1+x^2}}}, \tag{4}$$

where $y = (\sqrt{1+x^2} - 1)/x$, $x = 4\mu_{\rm B} B/\omega$ with $\mu_{\rm B}$ being the electron magnetic moment, $d = Q_{\rm Ps} V_{zz}$ and $\eta = |V_{xx} - V_{yy}/V_{zz}|$ are the Ps quadrupole coupling

constant and the asymmetry parameter of the EFG tensor, respectively, with the Ps effective quadrupole moment $Q_{\rm Ps}$ given by [14]

$$Q_{\rm Ps} = \frac{m_{\rm e} - m_{\rm p}}{m_{\rm e} + m_{\rm p}} \langle 3z^2 - r^2 \rangle. \tag{5}$$

Here, $m_{\rm e}$ and $m_{\rm p}$ are the effective masses of the electron and the positron, respectively, and $\langle \ldots \rangle$ denotes the quantum mechanical averaging of the quadrupole moment operator $3z^2 - r^2$ ($r = \sqrt{x^2 + y^2 + z^2} = |\boldsymbol{r}_{\rm e} - \boldsymbol{r}_{\rm p}|$ with $\boldsymbol{r}_{\rm e}$ and $\boldsymbol{r}_{\rm p}$ being the electron and positron radius–vectors, respectively) over the exact triplet ground state wave function taking the electron–positron hyperfine interaction into account.

The first attempt to measure the effective quadrupole interaction of Ps was reported in Ref. [16]. The sample was α-quartz where the Ps atoms are known to be delocalized (see, e.g., Fig. 2 where the satellite Ps peaks are clearly observed). For delocalized Ps state, the EFG tensor is axially symmetric with its $\boldsymbol{z}$ principal axis collinear with the $\hat{c}$ axis of the crystal and $\eta = 0$, so that only one quadrupole parameter, $d/\omega = d/\kappa\omega_0$, remains in Eq. (4) and Ξ in Eqs. (1) and (2) is φ independent. The anisotropy measured yields the ratio $d/\omega_0 \approx 0.16$ for $\kappa \approx 0.34$ reported recently in Ref. [17]. This is too large compared with the theoretical estimate $d/\omega_0 \approx 0.03$ [15]. The most probable reason of the disagreement may be the Doppler broadening method used, whose resolution is relatively poor, and a rather complicated way of the data analysis.

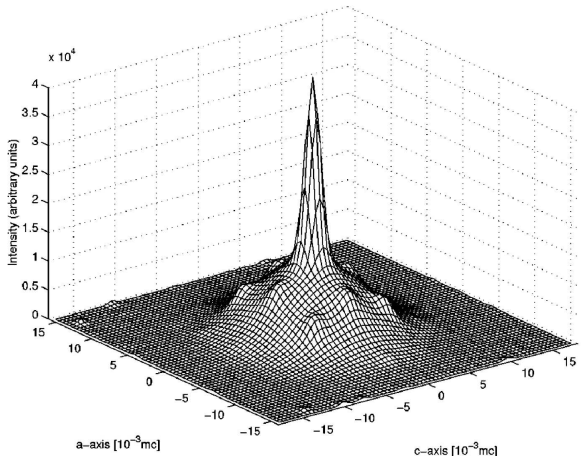

Fig. 2. Experimental 2D-ACAR spectrum of α-quartz at room temperature [2].

In Ref. [2], the intensity $I_{\rm Ps}(B, \theta)$ of the central Ps peak in α-quartz was measured using the 2D-ACAR method. Instead of changing the direction of the magnetic field, the sample was rotated by $\pi/2$ in the two different sets of measurements. It is to be noted that if one uses the 1D-ACAR method, the rotation of the

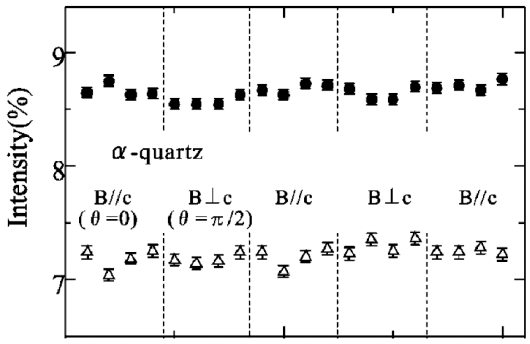

Fig. 3. Relative intensity of the Ps peak in α-quartz for the two different orientations of the sample with respect to the magnetic field direction [2]. Closed circles: $B = 1.25$ T, open triangles: $B = -0.25$ T.

sample leads to a change of the projection scanned of the Ps momentum distribution. Therefore, the 2D-ACAR method can only be used to correctly measure the anisotropy of the Ps peak intensity caused by the Ps quadrupole interaction. The intensity measured is represented in Fig. 3 for the two different magnetic fields and sample orientations with respect to the magnetic field direction. It clearly shows the existence of the quadrupole interaction of Ps in α-quartz. The quadrupole coupling constant has been determined to be $d = (3.0 \pm 0.9) \times 10^{-5}$ eV, yielding the ratio $d/\omega_0 \approx 0.038$ (for $\kappa \approx 0.34$ [17]) in agreement with the theoretical predictions of Ref. [15].

3.2. Ps–phonon scattering at elevated temperatures

In Sec. 2, it was pointed out that in most crystals the Ps atom was delocalized at low temperatures and tended to be self-trapped with increasing temperature. The only exceptions presently known are the crystals of MgF_2 and α-SiO_2 (α-phase of crystalline quartz). As is shown in recent experiments [18, 19], the Ps atom in these crystals remains delocalized up to temperatures ~ 700 K (this experimental fact was first explained theoretically in Ref. [7]). A typical experimental 2D-ACAR spectrum representing the 2D momentum distribution of delocalized Ps is shown in Fig. 2. The central and satellite peaks are broadened. This broadening is conventionally explained in terms of Ps scattering by long-wavelength longitudinal acoustic phonons. However, in MgF_2 a very drastic broadening of the central and satellite Ps peaks was observed at temperatures above 200 K, which was failed to be explained by Ps-acoustic-phonon scattering [18]. An effect appeared as if there were an additional scattering mechanism activated above 200 K which renormalized the acoustic deformation-potential constant of Ps so that it increased by a factor of approximately two in the narrow temperature range of 200–355 K. A similar effect was not observed in α-SiO_2 where the temperature broadening of the central and satellite peaks of the Ps momentum distribution was satisfactorily

explained by means of Ps-acoustic-phonon scattering throughout the entire temperature range of $\sim$ 80−700 K. In Ref. [19], an attempt was made to interpret the MgF_2 data above 200 K as the activation of the short-wavelength acoustic phonon scattering via umklapp processes. This mechanism was first discussed in Ref. [20]. However, such an explanation seems not to be quite satisfactory at least for the reason that it does not explain why the same effect is absent in α-SiO_2. In Ref. [3], it was shown that, though contributed to the renormalization of the acoustic deformation-potential constant, umklapp processes did not manifest themselves in the Ps momentum distribution measured experimentally.

In terms of the Green functions formalism [21], the linear projection experimentally measured of the momentum distribution (1D-ACAR spectrum) of the thermalized Ps atom interacting with phonons at finite temperatures is given by [18]

$$N(p_x) \sim \int_{-\infty}^{\infty} \mathrm{d}p_z \int_{-\infty}^{\infty} \mathrm{d}p_y \int_0^{\infty} \mathrm{d}\omega \mathrm{e}^{-\omega/k_\mathrm{B}T} \frac{\Gamma_{\boldsymbol{k}}(\omega)}{(\omega - \boldsymbol{p}^2/2M^*)^2 + \Gamma_{\boldsymbol{k}}^2(\omega)}, \tag{6}$$

where the exponential factor stands for the Boltzmann statistics because there is at most only one Ps atom at a time under usual experimental conditions. The non-exponential factor represents the so-called spectral density function in its explicit form with $\Gamma_{\boldsymbol{k}}(\omega)$ being the imaginary self-energy of Ps with the quasimomentum $\boldsymbol{k} = \boldsymbol{p}/\hbar$. The latter one is usually written to the lowest (second) order approximation in the Ps interaction with a phonon field:

$$\begin{aligned}\Gamma_{\boldsymbol{k}}(\omega) = \pi \sum_{\boldsymbol{q}} |V_{\boldsymbol{q}}|^2 [(n(\omega_{\boldsymbol{q}}) + 1)\delta(\omega - E_{\boldsymbol{k}+\boldsymbol{q}} - \hbar\omega_{\boldsymbol{q}}) \\ + n(\omega_{\boldsymbol{q}})\delta(\omega - E_{\boldsymbol{k}+\boldsymbol{q}} + \hbar\omega_{\boldsymbol{q}})],\end{aligned} \tag{7}$$

where $V_{\boldsymbol{q}}$ is the interaction matrix element, $E_{\boldsymbol{k}} = \hbar^2\boldsymbol{k}^2/2M^*$ is the energy of Ps with the band mass M^*, $n(\omega_{\boldsymbol{q}}) = [\exp(\hbar\omega_{\boldsymbol{q}}/k_\mathrm{B}T) - 1]^{-1}$ is the equilibrium phonon distribution function, and $\omega_{\boldsymbol{q}}$ is the frequency of the phonon with the wave vector $\boldsymbol{q}$.

The interaction energy of a particle with lattice vibrations in its simplest form depends linearly on strain — acoustic strain in the case of acoustic phonon modes and optic strain in the case of optic phonon modes (see, for instance, Ref. [22]). These strains influence the particle in its band in two distinct ways. In the first way, short-range disturbances of the periodic potential cause practically instantaneous changes in energy, and these are the ones quantified by deformation potentials and referred to as deformation-potential scattering (acoustic and nonpolar optic, respectively). In the second way, the distortion of the lattice may destroy local electric neutrality, and produce electric polarization and associated macroscopic comparatively long-range electric fields to which the particle responds. Disturbance of the particle's motion by this effect is referred to as piezoelectric scattering, if associated with acoustic modes, and polar optic scattering, if associated with optic modes. Contrary to deformation-potential scattering, the latter two

are believed to be less important for the Ps atom in ionic crystals because of its electric neutrality.

For the acoustic and optic deformation-potential scatterings, the imaginary self-energies are given from Eq. (7) by [3]

$$\Gamma_{\boldsymbol{k}}^{(\mathrm{a})}(\omega) = \frac{{E_\mathrm{d}}^2 M^{*3/2} k_\mathrm{B} T}{\sqrt{2}\pi\hbar^3 u^2 \rho}\sqrt{\omega} \tag{8}$$

and

$$\Gamma_{\boldsymbol{k}}^{(\mathrm{o})}(\omega) = \frac{D_\mathrm{o}^2 M^{*3/2}\sqrt{\omega}}{2\sqrt{2}\pi\hbar^2\rho\omega_\mathrm{o}}\left[(n(\omega_\mathrm{o})+1)\vartheta\left(1-\frac{\hbar\omega_\mathrm{o}}{\omega}\right)\sqrt{1-\frac{\hbar\omega_\mathrm{o}}{\omega}}\right.$$
$$\left. + n(\omega_\mathrm{o})\sqrt{1+\frac{\hbar\omega_\mathrm{o}}{\omega}}\right], \tag{9}$$

respectively. Here, E_d and D_o stand for the acoustic and optic deformation potential coupling constants, respectively, ρ is the density of the crystal, u is the average velocity of long-wavelength longitudinal acoustic vibrations, ω_o is the frequency of long-wavelength optic vibrations, $\vartheta(t)$ is the unit-step function, k_B is the Boltzmann constant. The total imaginary self-energy accounting for both acoustic and nonpolar optic Ps–phonon scatterings is then written as

$$\Gamma_{\boldsymbol{k}}(\omega) = \Gamma_{\boldsymbol{k}}^{(\mathrm{a})}(\omega) + \Gamma_{\boldsymbol{k}}^{(\mathrm{o})}(\omega) = \frac{\widetilde{E}_\mathrm{d}{}^2(\omega) M^{*3/2} k_\mathrm{B} T}{\sqrt{2}\pi\hbar^3 u^2 \rho}\sqrt{\omega} \tag{10}$$

with

$$\widetilde{E}_\mathrm{d}(\omega) = \left\{ {E_\mathrm{d}}^2 + \frac{\hbar u^2 D_\mathrm{o}^2}{2k_\mathrm{B}T\omega_\mathrm{o}}\right.$$
$$\left.\times\left[(n(\omega_\mathrm{o})+1)\vartheta\left(1-\frac{\hbar\omega_\mathrm{o}}{\omega}\right)\sqrt{1-\frac{\hbar\omega_\mathrm{o}}{\omega}} + n(\omega_\mathrm{o})\sqrt{1+\frac{\hbar\omega_\mathrm{o}}{\omega}}\right]\right\}^{1/2} \tag{11}$$

representing the "effective" deformation-potential constant with nonpolar optic scattering taken into account. In view of the fact that only $\omega \sim k_\mathrm{B}T$ mainly contributes to the Ps momentum distribution (6), the ω dependence of $\widetilde{E}_\mathrm{d}(\omega)$ can be approximately changed by T dependence. Then, $\widetilde{E}_\mathrm{d}(\mathrm{T})$ is easily seen to tend to E_d at $T \ll \hbar\omega_\mathrm{o}/k_\mathrm{B}$ and to $\widetilde{E}_\mathrm{d} = \sqrt{{E_\mathrm{d}}^2 + (uD_\mathrm{o}/\omega_\mathrm{o})^2}$ at $T \gg \hbar\omega_\mathrm{o}/k_\mathrm{B}$, explaining the results of the MgF_2 1D-ACAR experiment reported in Refs. [18, 19].

4. Second order phase transitions sensed by delocalized Ps

Figure 4 (left panel) shows the 1D-ACAR spectrum of Ps in MgF_2 calculated theoretically from Eqs. (6), (10), and (11) [3]. Optic deformation-potential scattering is seen to broaden the spectrum above 200 K in agreement with the experimental observations. This type of phonon scattering is known to be allowed

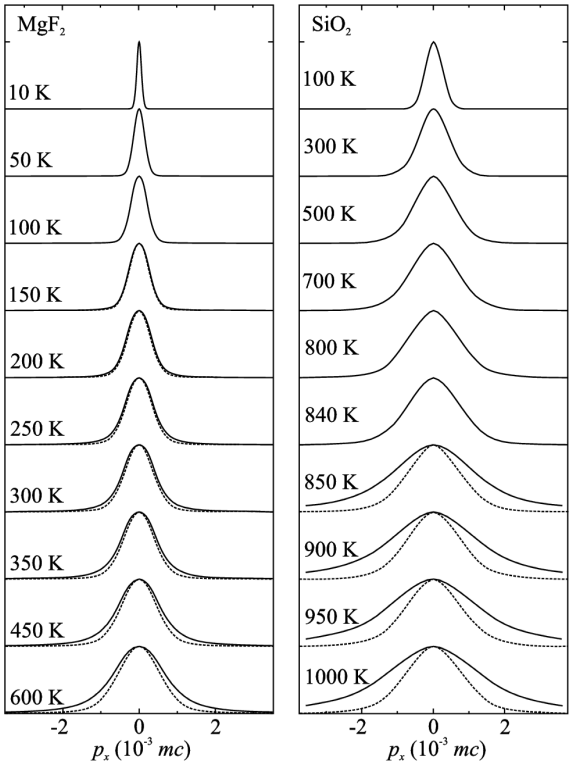

Fig. 4. Calculated central peaks of the Ps momentum distributions at different temperatures [3, 23]. Left panel: MgF_2, right panel: SiO_2. Solid and dashed lines represent the spectra with and with no optic deformation-potential scattering taken into account.

in degenerate and forbidden in nondegenerate Γ-valleys (Brillouin zone center) of cubic crystal lattices [22, 24]. The point is the constant D_{o} in Eq. (9) is the matrix element of the perturbation operator, that is the variation of the rigid-lattice potential due to optic lattice vibrations, taken over Bloch wave functions of a particle in the neighborhood of its band minimum [24]. For nondegenerate Γ-valleys of cubic lattices this matrix element transforms according to the unit representation of the point group of the crystal, whereas zone-center optic phonon modes are triply degenerate, i.e. they transform according to the three-dimensional group representation. As a consequence, the interaction energy with the optic deformation potential is not an invariant with respect to point group transformations and, therefore, vanishes ($D_{\mathrm{o}} \equiv 0$). If the point group of a crystal had lower symmetry than cubic (non-cubic crystals), then the three-dimensional group representation according to which zone-center optic phonon modes transform would be reducible. If this reducible representation contained irreducible one of the same dimensionality as the degeneracy multiplicity of the Γ-valley, then the optic modes transforming according to this irreducible representation would be present in the optic

deformation-potential interaction, thereby providing its invariance with respect to point group transformations. The constant $D_{\rm o}$ would be non-zero for such optic modes and they would scatter the particle in the Γ-valley.

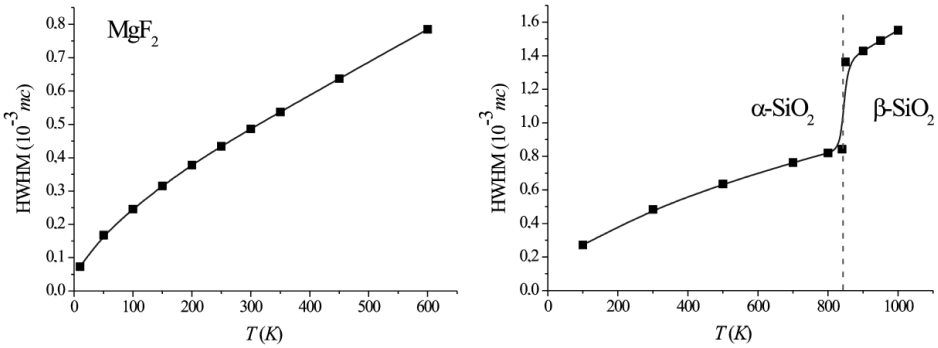

Fig. 5. Temperature dependences of HWHMs of the spectra in Fig. 4. Left panel: MgF_2, right panel: SiO_2.

An experimental evidence for the absence of an additional broadening mechanism of the Ps momentum distribution in α-quartz reported in Refs. [18, 19] can be interpreted as the fact that the optic deformation-potential scattering is forbidden in this crystal and the only Ps–phonon scattering mechanism is due to the acoustic deformation potential. However, crystalline quartz is known to undergo the second-order phase transition from α- to β-phase above 846 K [25]. In so doing, the type of the local symmetry of the quartz lattice changes from D_3 to D_6. A symmetry analysis done in Ref. [23] shows that, though forbidden in α-SiO_2, Ps nonpolar optic phonon scattering should manifest itself in β-SiO_2, giving rise to additional broadening of the Ps momentum distribution above 846 K. Figure 4 (right panel) represents the calculated temperature dependence of the 1D-ACAR spectrum in this case [23]. The Ps momentum distribution is seen to be drastically broadened in β-phase. Figure 5 compares the temperature dependences of the half widths at half maxima (HWHM) of the 1D-ACAR spectra in Fig. 4. The high-temperature $\alpha-\beta$ phase transition in SiO_2 manifests itself as a jump in the HWHM temperature dependence. This makes delocalized Ps a tool for investigation of high-temperature second-order structural phase transitions in those dielectric crystals where optic deformation-potential scattering is allowed in one and forbidden in another crystalline phase.

5. Conclusions

We have given a brief review of recent theoretical and experimental study of the Ps–phonon and Ps–quadrupole interactions in dielectric crystals of different local symmetries.

In crystal lattices of non-cubic symmetry, Ps may sense intracrystalline electric field gradients on it via an effective quadrupole moment it acquires due to the difference in effective masses of the electron and the positron. The Ps quadrupole interaction was recently detected in α-quartz. The effective quadrupole coupling constant of Ps was measured to be $(3.0 \pm 0.9) \times 10^{-5}$ eV in accordance with theoretical predictions. This shows that Ps spectroscopy can be applied to investigate anisotropic hyperfine interactions in solids.

Both in cubic and in non-cubic lattices, Ps interacts with local deformation potentials caused by phonons. Being a neutral particle, the Ps atom intensively interacts with short-range acoustic and optic deformation potentials only, not responding to long-range phonon-induced electric fields. As short-range deformation potentials are essentially symmetry dependent, Ps may be able to sense symmetry dependent structural properties of dielectric crystals. In particular, the high-temperature second-order phase transitions, where the local symmetry of the lattice changes but the crystalline structure remains, may be identified via jumps in the temperature dependences of HWHMs of Ps peaks measured in ACAR-experiments in those dielectric crystals where optic deformation-potential scattering is allowed in one and forbidden in another crystalline phase.

Acknowledgments

We would like to thank I.D. Feranchuk, L.V. Keldysh, L.I. Komarov, V.N. Kushnir, S.A. Kuten, Y. Nagai, H. Murakami, H. Saito, M. Sano, and N. Suzuki.

References

[1] T. Hyodo, *Mater. Sci. Forum* **363-365**, 233 (2001) and refs. therein.

[2] N. Suzuki, H. Saito, Y. Nagai, T. Hyodo, H. Murakami, M. Sano, I.V. Bondarev, S.A. Kuten, *Phys. Rev. B* **67**, 073104 (2003).

[3] I.V. Bondarev, *Phys. Lett. A* **291/1**, 39 (2001).

[4] K.P. Arefiev, O.V. Boev, S.A. Vorob'ev, P.V. Kuznetsov, *Fiz. Tverd. Tela* **26**, 1678 (1984) [*Sov. Phys. Solid State* **26**, 1017 (1984)].

[5] J. Kasai, T. Hyodo, K. Fujiwara, *J. Phys. Soc. Jpn.* **57**, 329 (1988) and refs. therein.

[6] I.V. Bondarev, T. Hyodo, *Phys. Rev. B* **57**, 11341 (1998).

[7] I.V. Bondarev, *Phys. Rev. B* **58**, 12011 (1998).

[8] V.G. Baryshevsky, S.A. Kuten, *Phys. Lett. A* **64**, 238 (1977).

[9] J.H. Brewer, D.S. Beder, D.P. Spencer, *Phys. Rev. Lett.* **42**, 808 (1979).

[10] V.B. Berestetskii, E.M. Lifshitz, L.P. Pitaevskii, *Quantum Electrodynamics*, Pergamon, Oxford 1982.

[11] C.P. Slicter, *Principles of Magnetic Resonance*, Springer-Verlag, New York 1980.

[12] V.G. Baryshevskii, *Phys. Status Solidi B* **124**, 619 (1984).

[13] I.V. Bondarev, S.A. Kuten, *Z. Naturforsch. A* **49**, 439 (1994).

[14] I.V. Bondarev, S.A. Kuten, *Acta Phys. Pol. A* **88**, 83 (1995).

[15] I.V. Bondarev, *Fiz. Tverd. Tela* **41**, 999 (1999) [*Phys. Solid State* **41**, 909 (1999)].

[16] Th. Gessmann, J. Major, A. Seeger, J. Ehmann, *Philos. Magn. B* **81**, 771 (2001).

[17] H. Saito, T. Hyodo, *Phys. Rev. Lett.* **90**, 193401 (2003).

[18] Y. Nagai, M. Kakimoto, H. Ikari, T. Hyodo, *Mater. Sci. Forum* **255-257**, 596 (1997).

[19] Y. Nagai, M. Kakimoto, T. Hyodo, K. Fujiwara, H. Ikari, M. Eldrup, A. Stewart, *Phys. Rev. B* **62**, 5531 (2000).

[20] I.V. Bondarev, *Pis'ma Zh. Éksp. Teor. Fiz.* **69**, 215 (1999) [*JETP Lett.* **69**, 231 (1999)].

[21] G.D. Mahan, *Many-Particle Physics*, Plenum, New York 1981.

[22] B.K. Ridley, *Quantum Processes in Semiconductors*, Clarendon, Oxford 1982.

[23] I.V. Bondarev, *Nucl. Instrum. Methods B* **221**, 230 (2004).

[24] G.L. Bir, G.E. Pikus, *Symmetry and Deformation Effects in Semiconductors*, Wiley, New York 1975.

[25] *American Institute of Physics Handbook*, Ed. D.E. Gray, McGraw-Hill, New York 1972.